Tellus (1991), *43A*, 68–80

Effects of varying winds and fjord run-off on the circulation in the Skagerrak

By JOHN A. JOHNSON, *School of Mathematics, University of East Anglia, Norwich NR4 7TJ, England*

(Manuscript received 22 May 1989; in final form 21 May 1990)

ABSTRACT

An unsteady stratified model of the Skagerrak is described. The model includes the trench along the Norwegian coast and the shelf on the Danish side and is driven by a combination of surface wind stress, outflow from the Kattegat and run-off from the rivers and fjords along the Norwegian coast. The seasonal variation of the run-off is described and incorporated into the numerical model. Certain wind and run-off conditions produce a general outflow in the trench. Other conditions induce an outflow by the coast with a counter-current in the centre of the trench. Recirculation often occurs near the Swedish coast.

1. Introduction

The Skagerrak in an interesting area of sea bordered by Denmark, Norway and Sweden. It is open to the North Sea at the western end and connected to the Baltic Sea outflow through the Belt Sea by the Kattegat. The bottom topography of the Skagerrak consists of a trench up to 600 m deep on the Norwegian side and a shallow bank on the Danish side with an average depth of only 50 m. The deep trench is part of the Norwegian Trench that follows the coast of Norway to the edge of the continential shelf in the northern North Sea.

The density distribution in the Skagerrak generally consists of a light shallow layer above deep denser water with a sharp pycnocline at about only 40 m depth. Some salinity sections across the Skagerrak are presented in Rodhe (1987). The pycnocline generally becomes less sharp as the coast is approached, as illustrated by Gjevik and Høst (1984). Due to fresh water run-off the haline stratification is present throughout the year. The thermal stratification changes sign during the course of the year and in winter, for example, the coastal current is much colder than the underlying water and may reach down to 100 m depth.

There are many different driving mechanisms for the flow in the Skagerrak. There is the seasonally varying outflow from the Baltic through the Kattegat and run off into the Kattegat from Danish and Swedish rivers giving a typical annual inflow into the Skaggerak of about 15,000 $m^3 s^{-1}$ or 473 km^3 per year according to figures given by Svansson (1975). The run-off from the Norwegian rivers into the Skagerrak is very seasonal with the maximum after the Spring snow melt. A typical mean annual average is about 2,000 $m^3 s^{-1}$ or 63 km^3 per year. These figures must be compared with estimates of the Skagerrak current of about 200,000 $m^3 s^{-1}$ or 6,300 km^3 per year in February to 500,000 $m^3 s^{-1}$ or 15,750 km^3 per year in November. Hence the flow in the Skagerrak must be largely a recirculation of water entering from the North Sea and leaving by the Norwegian Trench, but modified by local inflows and winds. The recirculation is discussed by Furnes et al. (1986) who claim that the incoming Atlantic water is mostly retroflected in the Norwegian Trench before it reaches the Skagerrak.

Some of the inflow from the North Sea comes along the Danish coast as the Jutland current. An estimate of the transport in this current has been given by Jensen and Jonsson (1987) as 150,000 $m^3 s^{-1}$. The recirculation in the Skagerrak is described in the context of an extension to the North Sea circulation in a review article by Eisma (1987).

The effect of wind forcing on the Skagerrak out-

flow is investigated by Aure and Saetre (1981) who describe the alteration between the blocking of the outflow by westerly winds and the outbreak of Skagerrak water that follows when the westerly winds relax. The outflowing water usually follows the Norwegian coast but it sometimes diverges from the coast and enters the North Sea, as shown by Saetre et al. (1988). Current measurements have been made along two sections in the Skagerrak by Rodhe (1987), showing a mainly cyclonic circulation. Gammelsrød and Hackett (1981) have used inverse methods to infer the geostrophic circulation in the Skagerrak at three sections from hydrographic data. They show that the dominant flow is a recirculation of water from the North Sea into the Norwegian Trench.

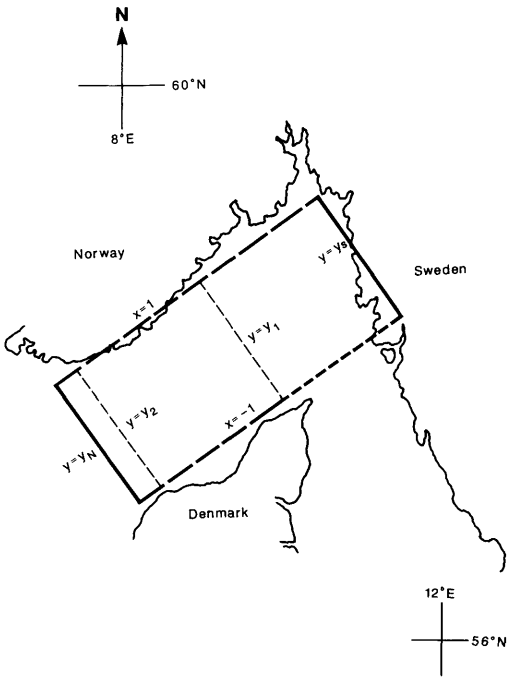

Fig. 1. The coordinate system of the model in relation to the Skagerrak.

2. The model formulation

In Johnson (1985a), a set of model equations are derived for the flow in a long narrow sea. These equations are solved for a model with trench topography and uniform coastal run-off in Johnson (1985b). In this paper, the solution is extended to include non-uniform run-off that represents the seasonal outflow from the Norwegian rivers, a deeper trench with a profile similar to the Skagerrak, and the effects of wind stress forcing at the surface. The derivation of the appropriate model equations is described in Section 4.

As the region of sea being modelled is of limited latitudinal extent the β-effect is unimportant and hence the Coriolis parameter f is assumed constant. Therefore the orientation of the axes is not significant from a latitudinal point of view and so they are chosen with y measured along the coast and with x as the onshore coordinate. This is in keeping with most other models of flows in coastal trenches and over continential shelves. The vertical coordinate z is upward from the surface at $z=0$. The coordinate system in relation to the Skagerrak is illustrated in Fig. 1. The Swedish coast lies at $y=y_s$ and the outflow to the North Sea at $y=y_N$.

The model described below is suitable for the narrow trench on the Norwegian side of the Skagerrak where the majority of river run-off enters the sea, and may be regarded as the first part of a much larger model that follows the Norwegian Trench around the coast. To simplify the calculations it is assumed that the bottom topography is given in dimensionless form by $z=-H(x)$ with a vertical end at the Swedish coast. This is clearly not a very satisfactory model near the Swedish coast but the main interest in this paper is the effect of the current downstream from the run-off from the Norwegian coast.

In the derivation of the model equations in Johnson (1985a) the principal requirments are that the velocity component v along the coast and along the trench is larger than the onshore component u, and that variations along the trench have a longer length scale than variations across the trench. This leads to considerably simplification in the differential equation to be solved for v. With the trench topography, the onshore interior transport is restricted in magnitude by the fact that it has to enter the bottom boundary layer on the sides of the trench, whereas the alongshore flow is unrestricted as the far end of the trench is open to the deep sea.

3. The run-off along the Norwegian coast

The principal run-off from the Norwegian coast into the Skagerrak comes from the following rivers, from east to west, Glomma, Dramselv, Numedalslogan, Skienselv and Nidelv. The mean monthly outflow from these rivers over the period 1971–1980 has been determined by the Norwegian Water Resources and Electricity Board (NVE) and is summarized in Fig. 2a. For each river there is a spring maximum in May following the snow melt. This is preceded by a minimum in March due to the locking up of water in ice and snow. The annual mean for each river is given in Table 1. The total annual average run-off from these five rivers for this period of years is 1,269 $m^3 s^{-1}$, which may be compared with the figure for typical run-off into the Skagerrak of 2,000 $m^3 s^{-1}$ given in Section 1.

Table 1.

River	*Annual mean outflow* ($m^3 s^{-1}$) (1971–1980)
Glomma	7300
Dramselv	3082
Numedalslogan	1162
Skienselv	2660
Nidelv	1026

This distribution of average run-off along the coast is represented in Fig. 2b.

As the main interests in this paper is the effect of run-off on the flow in the Skagerrak it is convenient to fit an analytical expression to this data to facilitate insertion in the numerical model. To include the annual variation, let the run-off along the coast be given by

$$R_F(y, t) = R_T(t)\, R_C(y), \tag{1}$$

where the temporal variation is represented by

$$R_T(t) = 4 + \tfrac{1}{2}\tanh 0.07(90 - t) + \tanh 0.05(t - 210) + \tfrac{1}{2}\tanh 0.07(370 - t) + 8\,\mathrm{sech}\, 0.05(t - 201), \tag{2}$$

where unit time corresponds to about one day. The distribution (2) is plotted in Fig. 3a against a monthly time scale and may be compared with the NVE figures for the five rivers in Fig. 2a. To allow for the variation along the coast for the various rivers an additional coastal function is included given by

$$R_C(y) = R_{FO}[\exp\{-120(y - y_s - 0.05)^2\} + 0.35\exp\{-120(y - y_1)^2\}] \tag{3}$$

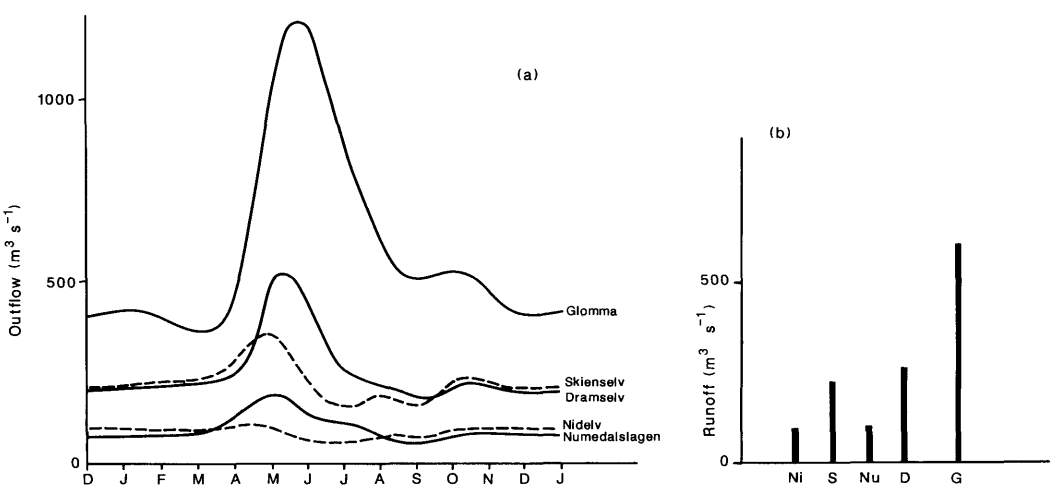

Fig. 2. (a) the annual variation in the mean monthly outflow from rivers into the Skagerrak. (b) The average run-off from each river per month. All data is based on the means from 1971 to 1980.

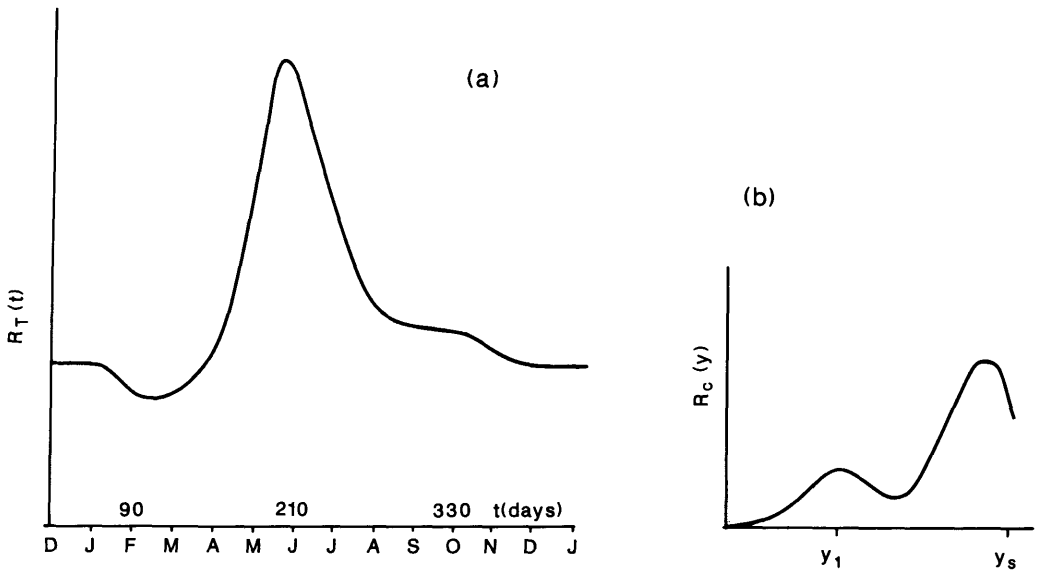

Fig. 3. The variation of (a) run-off with time, $R_T(t)$ given by eq. (2), (b) run-off along the coast, $R_c(y)$ given by eq. (3).

and shown in Fig. 3b, where R_{FO} and y_1 are constants. In all the numerical calculations that follow, $y_s = 0.8$, $y_1 = 1.1$, $y_2 = 1.4$ and $y_N = 1.5$.

The continuous distribution (3) is used to represent the general pattern of the discrete distribution of outflow from the rivers shown in Fig. 2b. The main interest in this paper is on the overall effect of run-off on the coastal current rather than the local effect near any individual estuary.

4. The equations of the model

The model cross-section is split into an interior region sandwiched between surface and bottom Ekman layers. In the interior region it has been shown in Johnson (1985a) that the dominant terms in the dimensionless equations of motion are

$$v = p_x, \tag{4}$$

$$(L/(lfT))\, v_t + u = -p_y, \tag{5}$$

$$p_z = S\theta, \tag{6}$$

$$u_x + v_y + w_z = 0, \tag{7}$$

$$(L/(TV))\, \theta_t + u\theta_x + u\theta_y + w\theta_z = 0, \tag{8}$$

where u, v and w are the velocity components corresponding to x, y and z, respectively, p is the pressure and θ is a buoyancy function (that includes the effects of salinity as well as temperature). Further details are given in the Appendix. Buoyancy function is used in place of the more comon equivalent temperature as the baroclinicity is more due to salinity than temperature. L and l are length scales related to the length and width of the Skagerrak, T is a time scale and V is a velocity scale, f is the local Corolis parameter and S is a stratification parameter.

The simplifications involved in eq. (4)–(8) may be summarized as follows. All frictional and diffusive effects are confined to the bottom and surface Ekman layers and only affect the interior region through Ekman suction. The hydrostatic balance (6) is a good approximation to the vertical distribution of p. As the Rossby number ($R_0 = V/fl$) is assumed small, the nonlinear terms in the momentum equations may be neglected compared with the geostrophic terms. The flow along the narrow sea is in geostrophic balance by eq. (4).

Two natural time scales appear in eq. (5) and (8). The shorter barotropic time scale, $T = T_1 = L/(lf)$, is associated with the spin up or geostrophic adjustment of the flow v along the narrow sea. The longer baroclinic time scale, $T = T_2 = L/V$, is concerned with the adjustments to the

buoyancy field due to advection. The ratio of T_1 to T_2 gives $T = R_0 T_2$.

The following are typical values for the Skagerrak; $l = 100$ km, $L = 300$ km, $V = 0.25$ m s^{-1}, $f = 10^{-4}$ s^{-1}. With these values the Rossby number $R_0 = 2.5 \times 10^{-2}$ and is indeed small. The barotropic time scale $T_1 = 8$ h, so that a significant change in the velocity field may be expected to happen over periods of a few days, with fairly rapid spin-up due to onset of wind. However, the baroclinic time scale $T_2 = 14$ days, which suggests that significant changes to the density or temperature and salinity fields are likely to occur more slowly over periods of 1 or 2 months.

The blocking situations described by Aure and Saetre (1981) are an almost instantenous reaction to a change in the westerly winds. These sudden changes are mainly confined to the surface Ekman layer, which in the model changes on a shorter time scale than T_1.

In order to deal with the rapid changes in the velocity field, choose $T = T_1$ so that (4) to (8) become

$$v = p_x, \qquad v_t + u = -p_y, \tag{9}$$

$$p_z = S\theta, \tag{10}$$

$$v_x + v_y + w_z = 0, \tag{11}$$

$$\theta_t + R_0(u\theta_x + v\theta_y + w\theta_z) = 0, \tag{12}$$

with the last equation demonstrating the slow changes in buoyancy function θ by advection with the rapidly changing velocity field.

To reflect the different time scales, let

$$p = p^*(x, y, t) + \hat{p}(x, y, z, R_0 t),$$

where p^* and $\hat{p}$ are the barotropic and baroclinic components of pressure respectively. Similarly let

$$u = u^* + \hat{u}, \qquad v = v^* + \hat{v},$$

but to allow for the variation of w with depth, let

$$w = w^*(x, y, z, t) + \hat{w}(x, y, z, R_0 t).$$

The buoyancy field is written

$$\theta = \hat{\theta}(x, y, z, R_0 t),$$

and changes only on the longer baroclinic time scale.

4.1. *The barotropic components*

Eqs. (9) to (11) are

$$v^* = p^*_x, \qquad v^*_t + u^* = -p^*_y,$$

$$p^*_\zeta = 0, \qquad H(u^*_x + v^*_y) + w^*_\zeta = 0, \tag{13}$$

where $\zeta = z/H(x)$ is a vertical coordinate that sets the surface at $\zeta = 0$ and the bottom at $\zeta = 1$. It may be deduced from (13) that

$$Hp^*_{xxt} = Hv^*_{xt} = w^*_\zeta \qquad \text{and} \qquad w^*_{\zeta\zeta} = 0. \tag{14}$$

The Ekman suction conditions, derived in Johnson (1985a), may be written

$$w^* = \tau^y_x - \tau^x_y \qquad \text{at} \qquad \zeta = 0, \tag{15}$$

and

$$w^* + H_x u^* = (\Lambda v^*)_x \tag{16}$$

at

$$\zeta = -1, \qquad \Lambda^2 = 2(1 + \lambda H_x^2),$$

where $\lambda = E_H/E$ is the ratio of the horizontal and vertical Ekman numbers, which is small for typical values appropriate to the Skagerrak. In eq. (15), the term $(-\tau^x_y)$ has been retained compared with Johnson (1985a). Here τ^x and τ^y are the wind stress onshore and alongshore, respectively. The retention of the τ^x_y term is to investigate the situation when the wind is blowing offshore from the Norwegian coast, that is for the case $\tau^x < 0$, $\tau^y = 0$. The second condition, eq. (16), states that the normal velocity into the bottom Ekman layer is proportional to the divergence of the Ekman transport (Λv^*).

Combining the suction conditions (15) and (16) with (14) leads to the eq. for the barotropic pressure field

$$Hp^*_{xxt} + H_x p^*_{xt} + p^*_{xx}\sqrt{2} + H_x p^*_y = \tau^y_x - \tau^x_y. \tag{17}$$

This eq. is solved subject to an appropriate set of boundary and initial conditions. The sea is closed by a boundary at $y = y_s$, corresponding to the Swedish coast, and therefore a condition of zero net transport through this boundary is satisfied if

$$p^* + \hat{p}|_{\zeta=-1} = \text{constant at} \quad y = y_s. \tag{18}$$

If $\tau^x \neq 0$ at $y = y_s$, then there is upwelling and

downwelling at this boundary. To avoid this complication in this investigation the wind stress τ^x is always chosen to have zero value at $y = y_s$.

At the Norwegian coast ($x = 1$) the boundary condition takes account of the volume input from the run-off as well as balancing the transports in the Ekman layers, which requires that

$$p_x^* + \hat{p}_x = v = (\tau^y + R_F)\sqrt{2} \quad \text{at} \quad x = 1, \tag{19}$$

where $R_F(y, t)$ is the coastal run-off or outflow from rivers and fjords described in Section 3. On the Danish side of the Skagerrak the water is generally shallow and, to simplify the calculations, a condition is applied over the Danish shelf that balances the transports towards the coast in the Ekman layers and in the interior so that

$$p_x^* + \hat{p}_x|_{\zeta=-1} + \left[H\sqrt{2}(p_y^* + p_{xt}^*) + \sqrt{2}\int_{-H}^{0} \hat{p}_y \, dz\right] = (\tau^y - R_K)\sqrt{2} \quad \text{at} \quad x = -1, \tag{20}$$

where $R_K(y, t)$ represents the outflow from the Kattegat near $y = y_s$. The bracketed terms on the left-hand side of (20) come from *Hu*, the interior transport.

To compute the barotropic solution requires integration of (17) starting from the initial condition $p^* = 0$ at $t = 0$ and satifying conditions (18) to (20). This provides the distribution of the barotropic velocity and pressure fields for $t > 0$ driven by surface wind stress $\underline{\tau}$, run-off R_F from rivers and fjords, outflow R_K from the Kattegat and feed-back from the baroclinic fields through $\hat{p}$ in (18) to (20).

4.2. *The baroclinic components*

The slowly varying baroclinic fields satisfy, from (9) to (12), the following eqs.

$$\hat{v} = \hat{p}_x - (\zeta H_x/H)\,\hat{p}_\zeta,$$

$$\hat{u} = -\hat{p}_y, \qquad \hat{p}_\zeta = SH\hat{\theta}, \tag{21}$$

$$\hat{u}_x - (\zeta H_x/H)\,\hat{u}_\zeta + \hat{v}_y + H^{-1}\hat{w}_\zeta = 0, \tag{22}$$

$$\hat{\theta}_t = -(u^* + \hat{u})(\hat{\theta}_x - \zeta H_x H^{-1}\hat{\theta}_\zeta) - (v^* + \hat{v})\,\hat{\theta}_y - (w^* + \hat{w})\,H^{-1}\hat{\theta}_\zeta, \tag{23}$$

where $\hat{t} = R_0 t$. At the initial time $t = 0$, the buoyancy function $\hat{\theta}(x, y, z, R_0)$ and hence, through (21), the pressure field $\hat{p}$ are prescribed. Subsequent variations in $\hat{\theta}$ are calculated using (23) and then the changes in $\hat{p}$, $\hat{u}$, $\hat{v}$, $\hat{w}$ are found using (21) and (22).

In the above formulation, it is assumed that the run-off enters at the local ambient density. This is a serious restriction (as only the effect of additional volume is included). However some interesting results are produced by this simplified model. A further investigation involving the run-off introducing its own buoyancy and the affects of advection in the boundary Ekman layers has been started.

5. The numerical solution

The numerical problem to be solved consists of the flow in a trench along a coast as shown in Fig. 4, with the flow driven by prescribed run-off R_F at the Norwegian coast at $x = 1$, by surface wind stress (τ^x, τ^y) and by prescribed outflow R_K from the Kattegat at $x = -1$ near $y = y_s$.

The barotropic pressure p^* is determined by solving (17) to (20) using a semi-implicit numerical method. In eq. (17), x derivatives are approximated by central differences whereas y and t derivatives are replaced by forward differences. Forward differences are used for y and t derivatives because of the nature of these terms in eq. (17). Central differences are used for x derivatives to give a more stable semi-implicit method. At $t = 0$, p^* is set equal to zero, the buoyancy distribution $\hat{\theta}$ is prescribed, and (21) is used to determine $\hat{p}$.

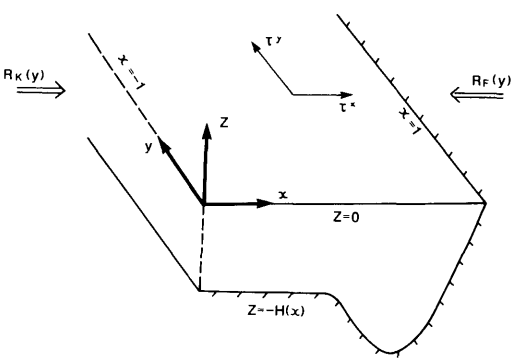

Fig. 4. Geometry of the model trench.

Using the latest values for $\hat{p}$ at each subsequent time-step t, the integration of (17) starts at $y = y_s$ and proceeds for increasing y using the Crank-Nicolson method to evaluate p^* at time step $t + \Delta t$ for all x-points across the Skagerrak for each y. The solution is stepped along the Skagerrak until $y = y_N$ is reached. When this is completed the calculation for p^* resumes at $y = y_s$ for time level $t + 2\,\Delta t$. The boundary conditions given by (19) and (20) with the most recent values of $\hat{p}$ are incorporated in the Crank-Nicolson tridiagonal matrix.

At each time step in the calculation, the slow change in $\hat{\theta}$ (and hence in $\hat{p}$) is determined from (23) using the latest values of u^*, v^*, w^* calculated from (13). The updated values of $\hat{p}$ are used to revise the values of $\hat{u}$, $\hat{v}$ and $\hat{w}$ using (21) and (22) which are then substituted in the next time step of the p^* calculation.

Special care has to be taken at the open boundary to the North Sea at $y = y_N$. When the flow is outward at $y = y_N$ there is no numerical problem. If however, the velocity at $y = y_N$ is inward with $V_N < 0$ then some decision has to be made about the buoyancy advected into the Skagerrak. It is assumed that changes occur more slowly in the open sea beyond $y = y_N$ than in the semi-enclosed Skagerrak. This assumption is built into the numerical scheme by arranging that, at one grid point beyond $y = y_N$, the buoyancy function is held fixed at the initial distribution (chosen at time $t = 0$) unless it is changed by (i) outward advection from the trench and shelf or (ii) slow sideways mixing. In mathematical terms these assumptions require the buoyancy θ_{N+1} at the grid point $y = y_{N+1}$ to satisfy

$$\frac{\partial \theta_{N+1}}{\partial t} = -\mu_1 R_0 V_N \frac{\partial \theta_{N+1}}{\partial y} + \mu_2 E_H \frac{\partial^2 \theta_{N+1}}{\partial x^2} \quad \text{if} \quad V_N < 0,$$

$$\frac{\partial \theta_{N+1}}{\partial t} = \mu_2 E_H \frac{\partial^2 \theta_{N+1}}{\partial x^2} \quad \text{if} \quad V_N > 0,$$

where μ_1 and μ_2 are constants and E_H is an Ekman number. The μ_1 terms represents the effect of outward advection and the μ_2 terms allows some lateral mixing. In the numerical calculations $\mu_1 = 4.0$ and $\mu_2 E_H = 0.05$.

In all the numerical examples described below, the following parameters are used

$$S = \tfrac{1}{2}, \qquad R_0 = 2.5 \times 10^{-2},$$

so that the baroclinic time scale is $40\times$ longer than the barotropic time scale. The time step $\Delta t = 0.02$ and the horizontal grid has $\Delta x = 0.067$ and $\Delta y = 0.05$ with 31 grid points across the Skagerrak and 15 grid points along the Norwegian coast. There are 11 grid points in vertical. The time step corresponds to about 30 minutes based on $t = 1$ corresponding to one day with a barotropic time scale of 8 h.

The wind stress distributions are, unless stated otherwise,

$$\tau^x = \tau_0^x \{1 - \exp(-2(y - y_s))\} \tanh 0.4t, \tag{24}$$

$$\tau^y = \tau_0^y \{1 - \exp(-2(y - y_s))\} \tanh 0.4t, \tag{25}$$

where τ_0^x, τ_0^y are specified constants. The tanh factor merely enables a smooth spin-up to the calculations. Note that the winds are zero at the "Swedish" coast at $y = y_s$. This avoids the complication with upwelling at that coast and is a numerical convenience. The initial buoyancy distribution is

$$\hat{\theta}(x, y, z, 0) = (\tfrac{1}{2} + \tfrac{1}{8} y) \times \{\tfrac{5}{8} + \tfrac{3}{8} \tanh 24(z + 0.15)\} \tag{26}$$

giving a lighter layer above $z = -0.15$ and a denser layer below with a smooth pycnocline around $z = -0.15$. Initially the buoyancy function increases (and the density decreases) with distance from the Swedish coast.

The outflow from the Kattegat is represented by

$$R_K = R_{KO}(y - y_s) \exp\{30(y_s - y)\} \tanh 0.4t, \tag{27}$$

where R_{KO} is a specified constant and the tanh term is again for smooth starting of the numerical calculation. As the principal purpose of this paper is to examine the effect of seasonal run-off from the Norwegian coast, a non-seasonal outflow from the Kattegat is used to avoid complicating the seasonal effect. The expression (27) effectively limits the outflow to the range $y_s \leqslant y \leqslant 0.7 y_1$ as illustrated in Fig. 8. This distribution (27) has an

appropriate cross-section to represent the Baltic current along the Swedish coast.

The bottom topography of the trench is specified by

$$H(x) = 0.15[1 + 5\exp\{-10(x-\tfrac{1}{3})^2\}] \times [1 - \exp\{10(x-1)\}], \quad (28)$$

which has a trench centred at $x = \frac{1}{3}$, just offshore of the "Norwegian" coast at $x = 1$, and a shelf as the "Danish" coast is approached at $x = -1$. The profile shape is shown in Fig. 4. The run-off from the Norwegian coast is given by (1) to (3) and represents, as described in Section 3, the annual variation of the run-off from the rivers and fjords of the eastern Skagerrak.

5.1. Example I. Reversing wind. No run-off.

The observations reported by Svansson (1975) and described in Section 1 imply that the effects of run-off are a perturbation to the main flow in the Skagerrak which is largely a recirculation of water entering from the North Sea. Therefore in this first example, run-off is excluded to illustrate the effect of changing wind direction on the basic Skagerrak circulation.

The wind stress distribution chosen for just this example is

$$\tau^x = -\{\tanh 2t - \tanh 2(t-10) + \tanh 2(t-14)\} \times \{1 - \exp(-2(y - y_s))\}, \quad (29)$$

$$\tau^y = 0,$$

which represents a change in the direction of the wind component τ^x at $t = 10$ and $t = 14$. An offshore wind ($\tau^x < 0$ at $t = 9$) produces a surface Ekman transport away from the Swedish coast at $y = y_s$, which is compensated by an inflow v in the interior as shown in Fig. 5. The interior v induces

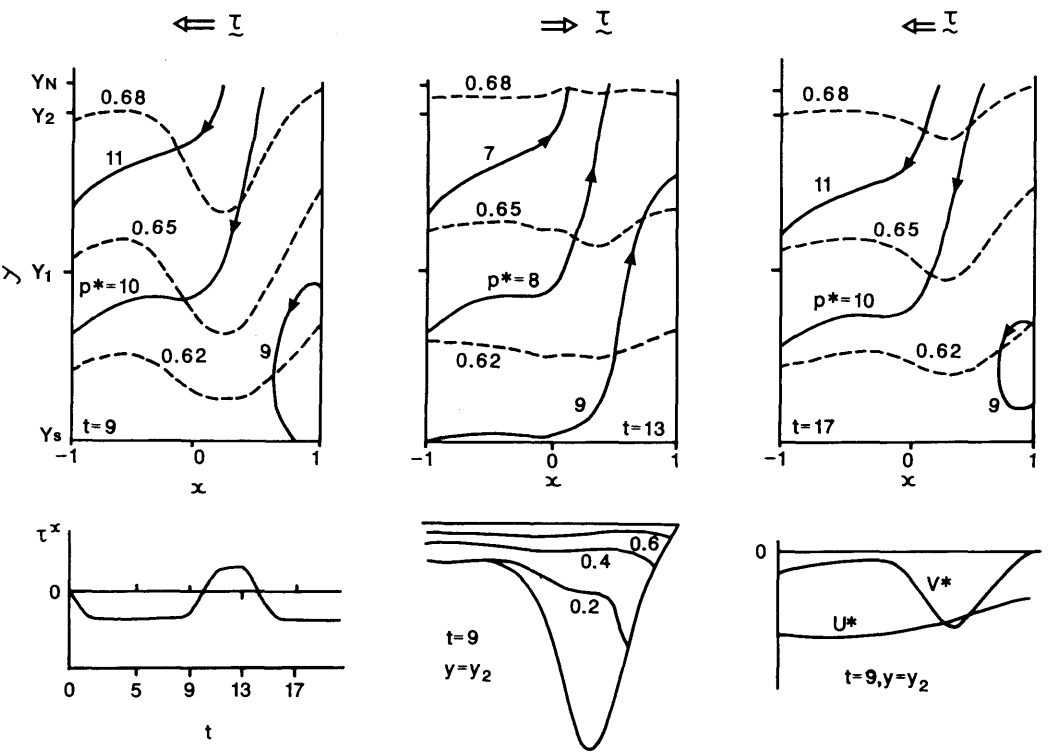

Fig. 5. Upper panels: Contours of p^* and θ_S (shown dashed) at times $t = 9$, 13, 17 for Example I with reversing wind and no run-off. Lower panels; left to right: (i) the variation of wind stress with time, (ii) the profile of bottom topography across the trench with isotherms at time $t = 13$, (iii) the distribution of v^* and u^* across the trench at time $t = 13$.

a flow towards the Norwegian coast in the bottom Ekman layer which in turn is compensated by a flow away from Norway in the interior. An onshore wind ($\tau^x > 0$ at $t = 13$) has the opposite effect and the interior flow is outward towards the North Sea. The contours for p^* provide an indication of the geostrophic components of the velocity field. As shown in (13) there is also an ageostrophic component when v^* is changing with time.

The main flow along the coast is in the centre of the trench with sometimes a weaker counter current near the coast. Cross-trench flows are stronger over the shelf due to the shallow depth and because the weaker alongshore flows over the shelf reduce the amount of onshore flow in the bottom boundary layer. The difference in the circulation when $\tau^x < 0$ with a westerly component of wind and when $\tau^x > 0$ with an easterly component of wind is consistent with the blocking effect on the circulation reported by Aure and Saetre (1981) when the wind is westerly. This effect will be discussed further in example III when the Kattegat outflow is included.

The isopycnals remain close together over the shelf showing the strong pycnocline but are more diffuse in the deeper water showing characteristic bowing in association with the along-trench velocity field. The isopycnals at the top of the interior region are advected back and forth by the interior flow.

5.2. *Example* II. *Seasonal run-off. No outflow from Kattegat*

The seasonal example includes the periodic run-off from the Norwegian coast discussed in Section 3 with $R_{FO} = 0.25$. To concentrate on the effect of various wind distributions on the circulation produced by this run-off, the effect of the outflow from the Kattegat is omitted from this example. For the case $\tau^x = 0$, $\tau^y < 0$ ($\tau_0^y = -0.5$ in (25))

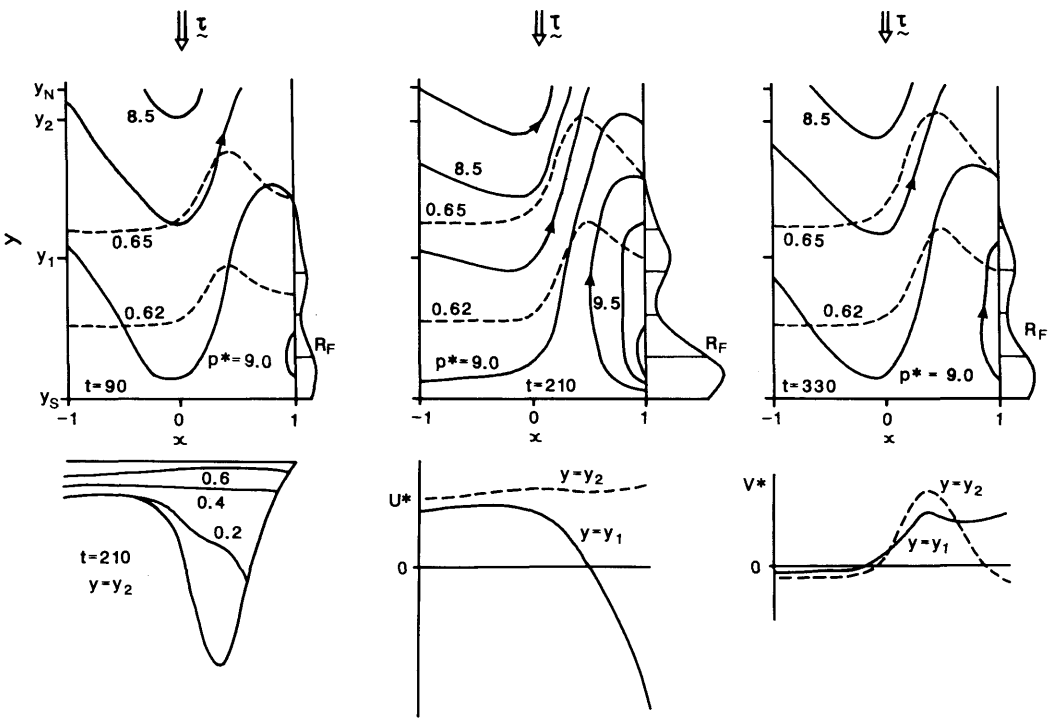

Fig. 6. Upper panels: Contours of p^* and θ_S (shown dashed) at times $t = 90$, 210, 330 for Example II with seasonal run-off R_F and no outflow from Kattegat. Lower panels; left to right: (i) the distribution of isotherms across the trench, (ii) the velocity v^* and (iii) the velocity u^*, all at time $t = 210$ and at position $y = y_1$ or $y = y_2$.

with the wind blowing into and along the Skagerrak, the numerical solution is illustrated in Fig. 6. The times $t = 90$, 210, 330 correspond to February, June and October respectively. June is the time of maximum run-off as seen in Fig. 3a whereas February is in the middle of the winter period of minimum run-off and October is at the end of the period of large spring and summer run-off.

With the wind stress into and along the Skagerrak, the surface Ekman transport is offshore from the Norwegian coast inducing a general onshore flow in the interior except when it is affected by the run-off. The inflow to the model caused by the run-off induces a net outflow from the Skagerrak to the open sea at $y = y_N$. The maximum outflows occurs over the trench at $y = y_2$ downstream of the river inflow, but at the coast at $y = y_1$ where there is run-off. The outflow is proportional to the amount of run-off and is greatest in June. Interpretation of these figures may be helped if it is recalled that although the dimensionless u and v have similar magnitudes, the corresponding dimensional u is much less than v due to the scaling used to obtain (9).

The shape of the isopycnals are very similar to the alongshore v velocity, indicating the importance of advection. The interesting bowing of the isopycnals with depth is associated with the complex u and v distributions. As surface heating and cooling are not included in this model, the seasonal effect of temperature is not apparent in these figures.

The effects of changes in wind direction on the circulation produced by the October run-off are shown in Fig. 7. Once again due to the net inflow from rivers and fjords there is a net interior outflow from the Skagerrak in all cases. However the outflow is not uniform across the channel. Three different wind directions are represented in

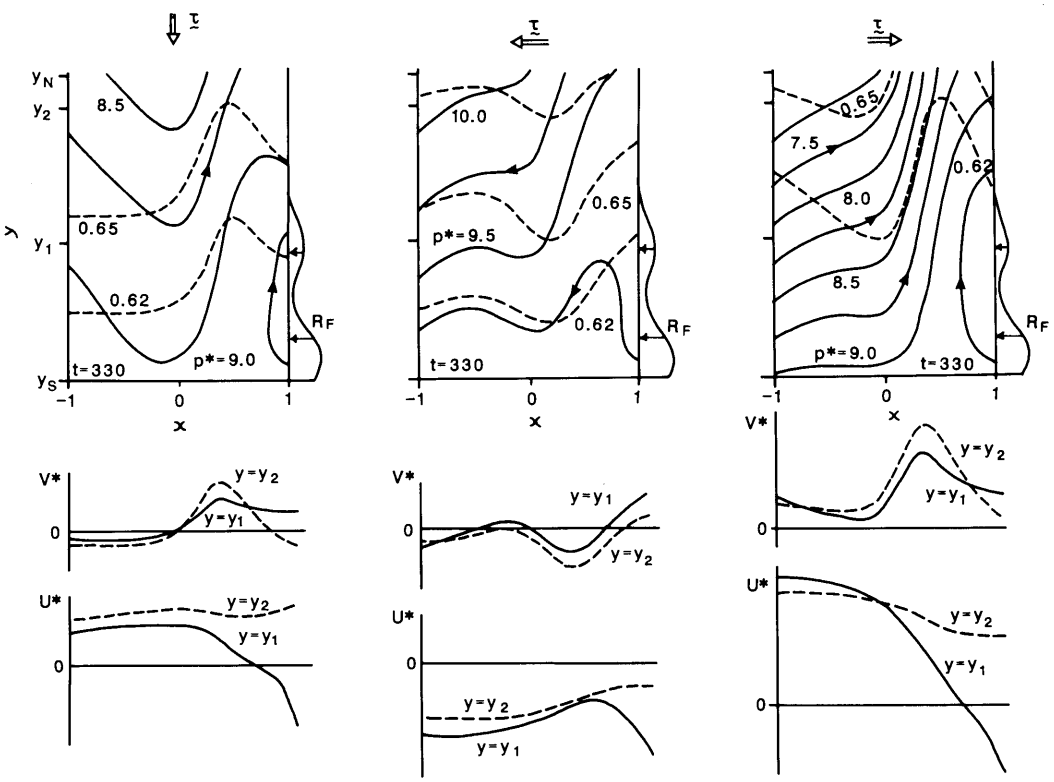

Fig. 7. Contours of p^* and θ_S and distribution of R_F, u^*, v^* for Example II with seasonal run-off and no outflow from Kattegat. From left to right the panels show at time $t = 330$ (corresponding to October) cases (a) $\tau_0^* = 0$, $\tau_0^y = -\frac{1}{2}$, (b) $\tau_0^x = -\frac{1}{2}$, $\tau_0^y = 0$, (c) $\tau_0^x = \frac{1}{2}$, $\tau_0^y = 0$.

Fig. 7 using the wind distribution (24) and (25) with (a) $\tau_0^x = 0$, $\tau_0^y = -\frac{1}{2}$; (b) $\tau_0^x = -\frac{1}{2}$, $\tau_0^y = 0$; (c) $\tau_0^x = \frac{1}{2}$, $\tau_0^y = 0$. In case (a) the wind is blowing into the Skagerrak from the south-west and generates a surface Ekman transport away from the coast at $x = 1$ towards the shelf at $x = 0$. This transport induces a positive u over the shelf whereas the run-off at $x = 1$ requires a negative u on that side of the channel. As there is no surface Ekman transport along the channel, the net outflow in the trench is provided by a combination of the return inflow over the shelf and the run-off along the coast.

For case (b) with a northwesterly wind blowing offshore from the coast at $x = 1$, the surface Ekman transport is along the channel towards the open sea. Thus the net outflow from the run-off is shared between the surface Ekman layer and the interior. Hence the interior transport is largely a recirculation with inflow from the open sea along the deeper part of the trench and outflow near the coast. This situation with a counter-current in the trench is similar to the observations described by Aure (1978) of a section across the Skagerrak off Stavern in November 1974.

The positive τ^x in case (c) represents a wind blowing from the south-east towards the Norwegian coast which induces a surface Ekman transport into the Skagerrak from the open sea. Therefore there must be a larger interior outflow than in the previous two cases to deal with both the incoming Ekman transport and the inflow from run-off. The interior u velocity balances the bottom Ekman transport induced by the positive v

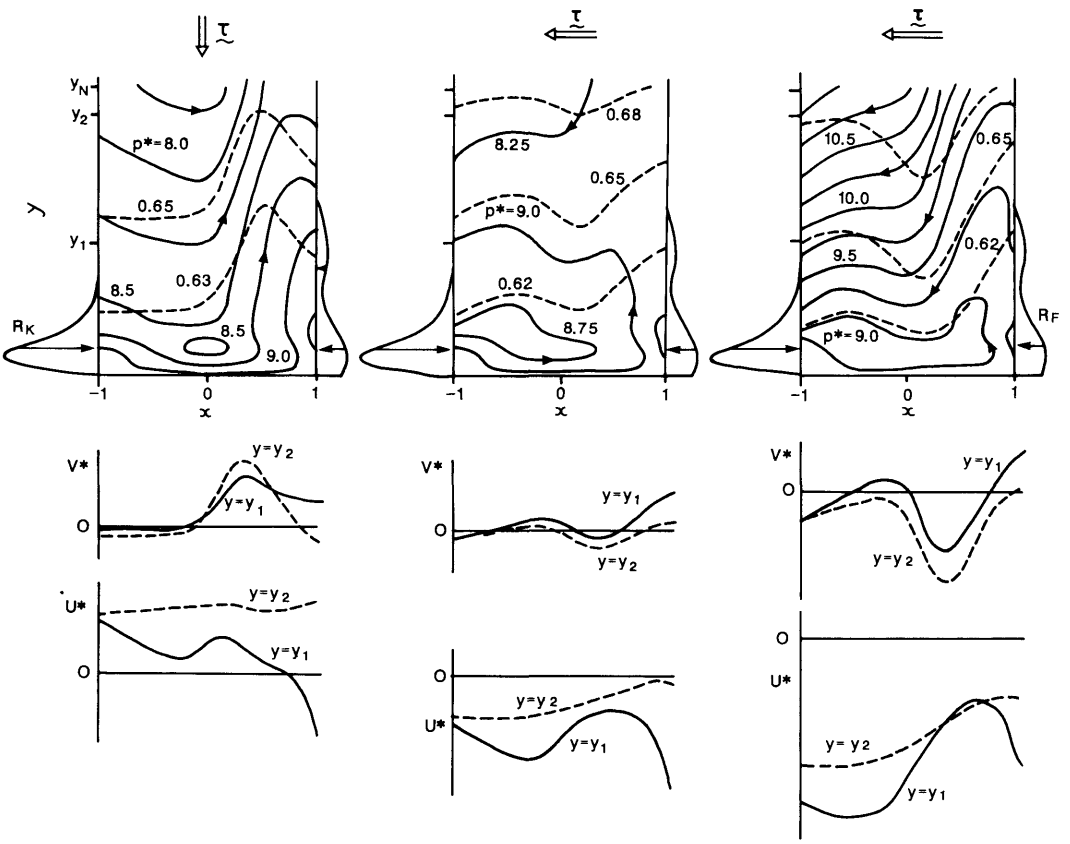

Fig. 8. Contours of p^* and θ_S and distributions of u^*, v^* for Example III with seasonal run-off R_F and outflow from Kattegat R_K. From left to right the panels show at time = 210 (corresponding to June) cases (a) $\tau_0^x = 0$, $\tau_0^y = -\frac{1}{2}$, (b) $\tau_0^x = -\frac{1}{2}$, $\tau_0^y = 0$, (c) $\tau_0^x = -1$, $\tau_0^y = 0$.

over the shelf near $x = -1$ and accepts the run-off at $x = 1$. For the same wind distribution but with increased run-off in June a similar circulation pattern is produced but with enhanced velocities. The peak in the outflow in the centre of the trench is similar to the observations described by Aure (1978) for a section across the Skagerrak off Jomfruland in June 1974.

5.3. *Example III. Seasonal run-off. Outflow from Kattegat*

In this example, a mean outflow R_K, given by (27), from the Kattegat is included, and the run-off R_F is reduced in magnitude compared with the previous example, giving a better balance between the two inputs of water into the Skagerrak. The coefficients $R_{KO} = 200$ and $R_{FO} = 0.15$ are chosen which gives a net outflow from the Kattegat that is about eight times the net run-off along the Norwegian coast in agreement with the relevant magnitude given in the introduction.

Three different wind vectors are considered with τ^x and τ^y given by (24) and (25) for (a) $\tau_0^x = 0$, $\tau_0^y = -\frac{1}{2}$; (b) $\tau_0^x = -\frac{1}{2}$, $\tau_0^y = 0$; (c) $\tau_0^x = -1$, $\tau_0^y = 0$. The numerical results are presented in Fig. 8 for $t = 210$ (corresponding to the June run-off). In case (a) the south-westerly wind blows into the Skagerrak from the open sea, similar to Fig. 7(a), and induces a surface Ekman transport away from the Norwegian coast. This is compensated by a general interior flow towards that coast. The along trench component v is strongest in the trench and is reversed over the shelf where it permits inflow in the bottom boundary layer. The distortion of the surface isopycnals indicate the strong advection in the trench.

The other cases both have the north-westerly wind blowing offshore from the Norwegian coast, but with different strengths, and with surface Ekman transport along the Skagerrak towards the open sea. In case (b) the surface Ekman transport is roughly equivalent to the inflow from run-off and from the Kattegat. Consequently the interior flow just recirculates and does not contribute significantly to the outflow. The negative v over the shelf is associated with an inflow in the bottom boundary layer. In case (c) the increased wind induces an increased outward surface Ekman transport and to compensate there is a net interior inflow from the open sea particularly along the trench with a coastal jet flowing out along the Norwegian coast. There is a significant recirculatory gyre near the Swedish coast at $y = y_s$. This circulation pattern is very similar to the observed flow described by Rodhe (1987) from observations taken in 1975 to 1977. Unfortunately no wind data is given.

6. Summary

Some of the effects of wind driving, river and fjord run-off and Kattegat outflow on the circulation of the Skagerrak have been considered. The examples described in Section 5 have concentrated on the changes to the flow in the Skagerrak caused by seasonal run-off from along the Norwegian coast, for various prescribed winds. No detailed examination has been made of the relative strengths of the circulation produced by winds and run-off, or of the considerable seasonal variations in the outflow from the Kattegat. To perform such a calculation adequately requires the use of a primitive equation model driven by a time series of wind distribution. This paper is concerned with using a simplified model to assess the qualitative effects of certain combinations of driving mechanisms.

From the examples in Section 5, it is apparent that if the wind is off the Norwegian coast (that is north-westerly) there is a strong inflow into the Skagerrak from the open sea within the trench with a weaker counter-current near the coast. This result is similar to the blocking effect described by Aure and Saetre (1981). Whereas when the wind is south-westerly or into the Skagerrak, the outflow is a maximum in the centre of the trench, as observed by Aure (1978). The overall pattern of the flow in the Skagerrak is the recirculation of water entering from the North Sea, but modified by inflows from the Kattegat and from the Norwegian rivers, often with a closed gyre near the Swedish coast. This mainly cyclonic circulation has been observed by Rodhe (1987).

7. Acknowledgments

My thanks are due to Professor B. Gjevik for arranging my visits to the Mathematics Institute at the University of Oslo for collaborative research sponsored by NATO Research Grant No. 84/0453.

8. Appendix

The relationships between the dimensionless (unstarred) variables and the dimensional (starred) variables are

$$x^* = lx, \qquad y^* = Ly,$$

$$z^* = (lD/L)z, \qquad t^* = Tt,$$

$$u^* = (lV/L)u, \qquad v^* = Vv, \qquad w^* = (lDV/L^2)w,$$

$$p^* + \rho_0 g z^* = (\rho_0 fVl)\, p,$$

$$\theta^* = \theta_0 + (\Delta\theta)\theta,$$

$$\rho^* = \rho_0[1 - \alpha(\theta^* - \theta_0)].$$

Here l, L, D are length scales related to width, length and depth of the Skagerrak respectively. V is a velocity scale and T a time scale. ρ_0 and θ_0 are constant reference density and buoyanct function respectively. $\Delta\theta$ is a scale for the vertical variation of buoyancy.

The dimensional buoyancy function θ^* is defined by

$$\alpha\theta^* = \alpha(\text{temperature}) - \bar{\alpha}(\text{salinity}),$$

where α is the coefficient of thermal expansion and $\bar{\alpha}$ is the fractional increase in density per unit increase in salinity. Substitution for p^*, z^* and ρ^* in the hydrostatic balance

$$\frac{\partial p^*}{\partial z^*} = -\rho^* g,$$

where g is the acceleration due to gravity, leads to

$$\frac{\partial p}{\partial z} = S\theta,$$

where $S = g\alpha D(\Delta\theta)/(f_0 VL)$ is a stratification parameter.

REFERENCES

Aure, J. 1978. The cooperative project "*The Norwegian Coastal Current*" Den Norske Kyststrøm Rapport 1/78. In Norwegian.

Aure, J. and Saetre, R. 1981. Wind effects on the Skagerrak outflow. In: *The Norwegian Coastal Current* (eds. R, Saetre and M, Mork) Bergen., pp. 263–293.

Eisma, D. 1987. The North Sea: an overview. *Phil. Trans. R. Soc. B316*, 461–485.

Furnes, G. K., Hackett, B. and Saetre, R. 1986. Retroflection of Atlantic Water in the Norwegian Trench. *Deep-Sea Res. 33*, 247–265.

Gammelsrød, T. and Hackett, B. 1981. The circulation of the Skagerrak determined by inverse methods. In: *The Norwegian coastal current* (eds. R. Saetre and M. Mork), Bergen, pp. 311–330.

Gjevik, B. and Høst, S. W. 1984. Long-crested internal waves in the Skagerrak. *Naturen 6*, 209–214. In Norwegian.

Jensen, T. G. and Jonsson, S. 1987. Measurement and analysis of currents along the Danish West Coast. *Dt. Hydrogr. Z. 40*, 192–213.

Johnson, J. A. 1985a. A stratified model of a partially enclosed narrow sea. *Geophys. Astrophys. Fluid Dynamics 32*, 61–90.

Johnson, J. A. 1985b. A stratified model of flow in a coastal trench. *Appl. Math. Modelling 9*, 403–408.

Rodhe, J. 1987. The large-scale circulation in the Skagerrak; interpretation of some observations. *Tellus 39A*, 245–253.

Saetre, R., Aure, J. and Ljøen, R. 1988. Wind effects on the lateral extension of the Norwegian Coastal Water. *Cont. Shelf Res. 8*, 239–253.

Svansson, A. 1975. Physical and chemical oceanography of the Skagerrak and Kattegat. *Report 1, Fish. Bd. Sweden, Inst. Mar. Res.*